

integration extends over the absorption band in question.  $\tau_0$  is the mean natural lifetime and is related to the observed lifetime,  $\tau$ , by the quantum yield of fluorescence:  $\tau = \tau_0\phi_f$ . We use eq 20 to estimate whether the lifetime corresponds to a single transition in the lowest absorption band or whether it is composed of two transitions according to the resolution made (Figure 6). The quantum yield and the observed lifetime for wye in water is determined to be  $\phi_f = 0.16$  and  $\tau = 4.3$  ns, respectively. This lifetime should be compared to 3.2 and 14 ns calculated using one or two transitions, respectively, in the lowest absorption band.

The first absorption band of wye can be described by two intensity components with polarizations according to Table I. However, since both the fluorescence lifetime measurement and the MCD are consistent with a single electronic transition, and also the polarization experiments (LD/FPA) can be explained with vibronic coupling, we suggest that the two absorption components belong to the same electronic origin ( $S_0 \rightarrow S_1$ ).

**Concluding Remarks.** The combination of UV dichroic and fluorescence polarization data on wye has permitted detailed conclusions as to moment directions and energies of the electronic transitions of this chromophore. In contrast to the common nucleic bases, wye displays a substantial fluorescence quantum yield which has been exploited in studies of structure, interactions, and mobility

in the anticodon loop of tRNA. The present information about the electronic states of wye can be anticipated to become of importance in this connection, since knowledge of the electronic transitions and their electric transition dipole moments is needed for the interpretation of essential features, such as energy transfer, repolarization, etc., in the fluorescence studies.<sup>37</sup> Such knowledge is also of crucial importance when interpreting linear and circular dichroism of nucleic acids in conformational terms;<sup>38,39</sup> the fact that wye absorbs at longer wavelength than the normal DNA bases might thus be used for selectively studying the structure at sites where this chromophore has been inserted as a probe. Finally, this study should also be considered in a general photophysical context aiming toward a fundamental understanding of the electronic properties of nucleic acid bases where, for instance, the question why the DNA bases do not fluoresce is an intriguing issue.

**Acknowledgment.** We are grateful to Prof. J. Chattopadhyaya for providing us with samples of wye and derivatives. The project is supported by the Swedish Natural Science Research Council.

(37) Claesen, F.; Rigler, R. *Eur. Biophys. J.* **1986**, *13*, 331.

(38) Matsouka, Y.; Nordén, B. *Biopolymers* **1982**, *21*, 2433.

(39) Matsouka, Y.; Nordén, B. *Biopolymers* **1983**, *22*, 1731.

## Ultraviolet Absorption Cross Sections and Atmospheric Photodissociation Rate Constants of Formaldehyde

Jerry D. Rogers

*Environmental Science Department, General Motors Research Laboratories, Warren, Michigan 48090-9055*  
(Received: October 5, 1989; In Final Form: January 10, 1990)

Ultraviolet absorption cross sections of gas-phase formaldehyde were measured over the wavelength range of 235–365 nm using a Bomem Fourier transform spectrometer. The uncertainties in the measured cross sections were 1–2%, including the estimated effect of systematic errors. The sum of the cross sections in the wavelength region between 300 and 365 nm was about 6% larger than the previous best estimate of this sum. These new UV cross sections were used to calculate photodissociation rate constants for formaldehyde for the  $\phi_1$  photolysis channel ( $\text{HCHO} \rightarrow \text{H} + \text{HCO}$ ) and the  $\phi_2$  photolysis channel ( $\text{HCHO} \rightarrow \text{H}_2 + \text{CO}$ ) at solar zenith angles ranging from 0° to 86°. The new photodissociation rate constants were about 8% larger for the  $\phi_1$  channel and about 10% smaller for the  $\phi_2$  channel than the currently accepted values for these rate constants.

### Introduction

The main reaction pathway for formaldehyde in the atmosphere is photolysis by ultraviolet radiation. There are two photolysis channels: (1) photolysis to produce HCO and an  $\text{HO}_2$  radical, in the presence of oxygen, and (2) photolysis to produce CO and  $\text{H}_2$ .<sup>1</sup> The HCO radical formed in the first photolysis channel of formaldehyde decomposes to CO and another  $\text{HO}_2$  radical; this channel is a major source of free radicals in urban areas and is thus important in determining the amount of ozone formed.

The rate of photolysis of formaldehyde in the atmosphere is directly proportional to the UV absorption cross sections of formaldehyde. McQuigg and Calvert<sup>2</sup> made the first definitive measurements of the UV absorption cross sections for formaldehyde. On the basis of those measurements, Baulch et al.<sup>3</sup> recommended a set of UV absorption cross sections for formaldehyde averaged over 10-nm intervals for use in modeling atmospheric chemistry. The UV absorption cross sections were subsequently remeasured at higher resolution by Bass et al.<sup>4</sup> and

by Moortgat et al.<sup>5</sup> The cross sections measured by these two groups were 25–50% lower than those measured by McQuigg and Calvert.<sup>2</sup> For wavelengths greater than about 300 nm, the cross sections reported by Bass et al.<sup>4</sup> were about 30% lower than those of Moortgat et al.<sup>5</sup> Baulch et al.<sup>6</sup> then changed the recommended UV absorption cross sections to the mean of the cross sections reported by Bass et al.<sup>4</sup> and by Moortgat et al.<sup>5</sup> These recommendations are still in use, although the uncertainty in the data is about  $\pm 35\%$ .<sup>7</sup>

The purpose of this work was to remeasure the UV absorption cross sections of formaldehyde and to use these results to calculate new photodissociation rate constants for formaldehyde. The UV

(4) Bass, A. M.; Glasgow, L. C.; Miller, C.; Jesson, J. P.; Filkin, D. L. *Planet. Space Sci.* **1980**, *28*, 675.

(5) Moortgat, G. K.; Klippel, W.; Mobus, K. H.; Seiler, W.; Warneck, P. "Laboratory Measurements of Photolytic Parameters for HCHO"; FAA Report FAA-EE-80-47, US Department of Transportation, Office of Environment and Energy: Washington, DC, November 1980.

(6) Baulch, D. L.; Cox, R. A.; Crutzen, P. J.; Hampson, R. F., Jr.; Kerr, J. A.; Troe, J.; Watson, R. T. *J. Phys. Chem. Ref. Data* **1982**, *11*, 327.

(7) DeMore, W. B.; Margitan, J. J.; Molina, M. J.; Watson, R. T.; Golden, D. M.; Hampson, R. F.; Kurylo, M. J.; Howard, C. J.; Ravishankara, A. R. *Chemical Kinetics and Photochemical Data for Use in Stratospheric Modeling*; JPL Publication 87-41; Jet Propulsion Laboratory, California Institute of Technology: Pasadena, CA; 1987.

(1) Atkinson, R.; Lloyd, A. C. *J. Phys. Chem. Ref. Data* **1984**, *13*, 315.

(2) McQuigg, R. D.; Calvert, J. G. *J. Am. Chem. Soc.* **1969**, *91*, 1590.

(3) Baulch, D. L.; Cox, R. A.; Hampson, R. F., Jr.; Kerr, J. A.; Troe, J.; Watson, R. T. *J. Phys. Chem. Ref. Data* **1980**, *9*, 295.

absorption cross sections of formaldehyde were measured between 230 and 370 nm using Fourier transform spectroscopy. The uncertainty in these cross sections is estimated to be about 1–2%. Photodissociation rate constants for the  $\phi_1$  channel ( $\text{HCHO} \rightarrow \text{H} + \text{HCO}$ ) and the  $\phi_2$  channel ( $\text{HCHO} \rightarrow \text{H}_2 + \text{CO}$ ) were calculated as a function of zenith angle, using these new UV absorption cross sections.

### Experimental Section

Gas-phase formaldehyde was generated by heating paraformaldehyde (Aldrich) in a glass vacuum system and condensing the vapor in a liquid nitrogen cooled trap. The formaldehyde was purified by a trap-to-trap distillation. No impurities were detected in either the infrared (IR) or ultraviolet (UV) spectra of the final product.

Ultraviolet absorption spectra of formaldehyde were measured on a Bomem DA 3.15 Fourier transform infrared spectrometer (FTIR) equipped with a Hamamatsu L 1403 deuterium UV lamp and a silicon/UV detector to extend the spectral range into the UV region. The absorption region of formaldehyde between 235 and 365 nm was isolated with a Corning No. 7-54 filter. A 99-cm-long by 4.6-cm-diameter Pyrex gas cell fitted with  $\text{CaF}_2$  windows was used for the measurements; this cell was connected directly to a glass vacuum system with Teflon tubing. Normally, the UV source is mounted on an external port of the Bomem spectrometer; however, in this work, the UV source was positioned 1.5 m from the external port. A 15 cm focal length mirror was used to collimate the UV beam and to direct it first through the 99-cm cell and then into the spectrometer.

Survey spectra of formaldehyde were measured with resolutions ranging up to 0.2 nm. For the absorption cross section measurements, resolutions of 0.011 and 0.044 nm were used. The absorption cross sections measured at 0.2-nm resolution were slightly smaller than those measured at the higher resolutions, but no effect of resolution on the measured cross sections was discernible between 0.01- and 0.04-nm resolution.

Ultraviolet spectra of a total of 44 samples of formaldehyde ranging from 0.8 to 9 Torr were used to calculate UV cross sections. Of these, 21 were at formaldehyde pressures less than 3 Torr, and 15 were at formaldehyde pressures less than 2 Torr. Measurements were made at  $296 \pm 2$  K.

Pressures were measured with either an MKS 310BHS 0–10-Torr head or an MKS 310CA 0–1000-Torr-head capacitance manometer, depending on the pressure. Both pressure heads agreed for differential pressure readings of formaldehyde to better than 0.3%. Although the absolute accuracy of these manometers is specified to be less than 0.1%, we conservatively estimate the absolute error in the pressure measurements to be about 1–2%, based on comparisons of readings between 1000-Torr head and a mercury manometer.

A potential error in these measurements is photolysis of the formaldehyde by the UV lamp. Such photolysis was found to be negligible even after 2 of continuous irradiation of the formaldehyde samples, since the spectra showed no change after this length of time. Nevertheless, a shutter was used to block the UV radiation from the samples until spectra were measured. The measurement time was about 5–10 min.

The effect of pressure broadening on the measured cross sections was examined by pressurizing formaldehyde contained in a 10-cm-long by 4.6-cm-diameter cell to atmospheric pressure with hydrocarbon-free air (Scott). The pressure of formaldehyde in these experiments ranged from 5 to 12.2 Torr. Spectra were measured by placing the 10-cm cell in the sample compartment of the Bomem spectrometer. Because some of the gaseous formaldehyde polymerized on the cell walls when the air was added, concentrations of formaldehyde were determined by measuring infrared spectra of the gas mixtures. To do this, several infrared spectra were first measured using a mercury cadmium telluride detector. Then, the beamsplitter, source, and detector of the spectrometer were changed to UV operation and several UV spectra were taken. Finally, more IR spectra were taken. The concentrations were calculated from the infrared spectra by using

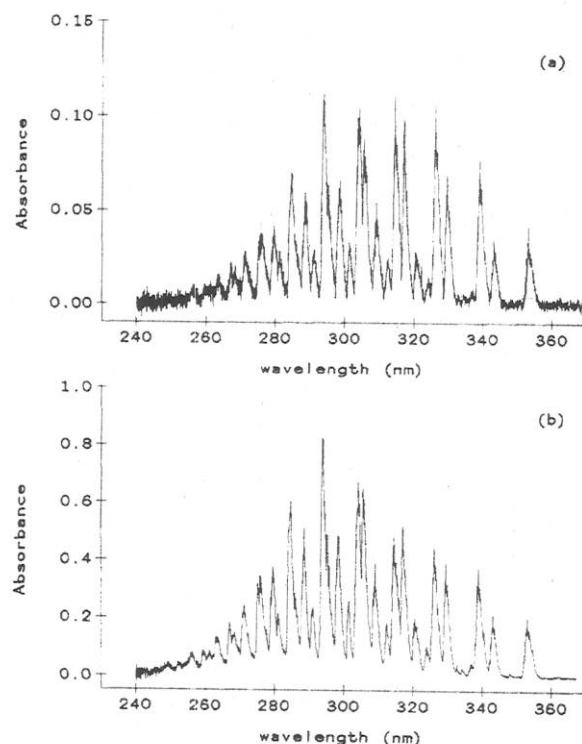


Figure 1. Ultraviolet absorption (base 10) spectra of formaldehyde: (a) 0.93 Torr and (b) 7.98 Torr. The path length was 99 cm, and the spectra were measured at a resolution of 0.044 nm.

the infrared band intensities of formaldehyde reported by Nakanaga, Kondo, and Saeki;<sup>8</sup> they estimate the accuracy of their measurements to be about 3%. From a plot of these concentrations vs time, the concentrations of formaldehyde at the time of each UV spectrum was estimated.

### Results

Ultraviolet spectra are shown in Figure 1a and Figure 1b for 0.93 and 7.98 Torr of formaldehyde, respectively. The absorbances for wavelengths longer than 300 nm were not linear with pressure for pressures greater than about 3 Torr. This effect can be seen by comparing Figure 1a for a formaldehyde pressure of 0.93 Torr with Figure 1b for a formaldehyde pressure of 7.98 Torr. These figures show that the absorbances at wavelengths longer than about 300 nm relative to those at wavelengths shorter than about 295 nm are smaller at the higher formaldehyde pressure.

Figure 2 shows an example of a plot of the average cross section vs pressure for the 10-nm wavelength interval from 325 to 335 nm. Both the UV cross sections calculated from direct pressure measurements and the UV cross sections calculated from the combined infrared and UV data are included. The formaldehyde pressures for the combined IR and UV data were obtained by using the infrared spectra to determine the pressure of formaldehyde in the 10-cm cell. Because the path length was 99 cm for the direct pressure measurements and 10-cm for the combination of UV and infrared measurements, the cross sections plotted in Figure 2 were divided by the path length to obtain a common comparison basis. The line shown in Figure 2 is the least-squares fit to only the 325–335-nm UV cross section measurements for which the pressure was less than 2 Torr. There were 15 such samples. The data from the combination of UV and infrared measurements are not included in the fit, because of the large amount of scatter caused by the small UV absorbances measured with the 10-cm cell. This short cell length was dictated by the physical size of the sample compartment of the FTIR spectrometer.

To eliminate the nonlinearity problem, the spectrum of formaldehyde was divided into three regions for determining the ab-

(8) Nakanaga, T.; Konda, S.; Saeki, S. *J. Chem. Phys.* **1982**, *76*, 3860.

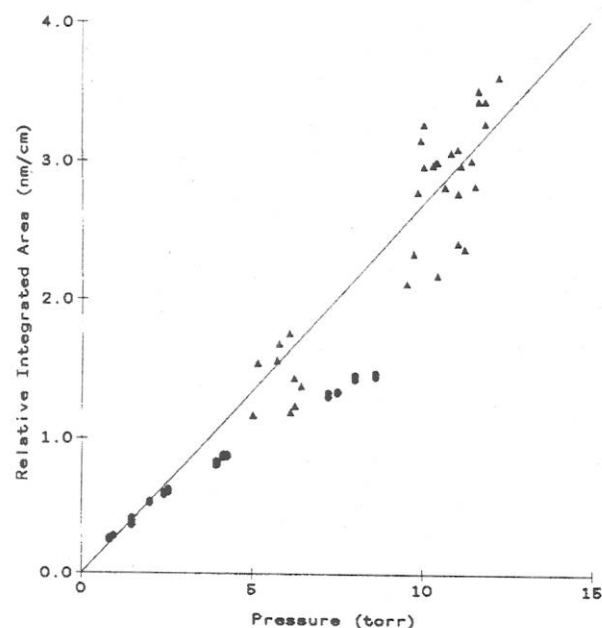


**Figure 2.** Integrated area of the 325–335-nm region of HCHO vs pressure. Both UV-only measurements (●) with no diluent gas and combined UV/IR measurements (▲) at 1-atm total pressure are included. The integrated area (base 10) was divided by the path length to obtain a relative integrated area. The line is the least-squares fit to the data for which the pressure was less than 2 Torr.

**TABLE I: Peak Cross Sections of Formaldehyde**

wavelength peak, nm	$10^{20}\sigma_e$ , cm <sup>2</sup> molecule <sup>-1</sup>			
	this work <sup>a</sup>	Moortgat et al. <sup>5</sup>	McQuigg and Calvert <sup>2</sup>	Bass et al. <sup>4</sup>
263.47	0.99	1.0	<i>b</i>	1.2
267.25	1.4	1.3	<i>b</i>	1.6
268.25	1.3	1.1	<i>b</i>	1.5
271.36	2.1	1.8	2.0	2.4
276.26	2.8	2.4		
276.65	2.1	2.5	{ 2.6	{ 3.5
279.76	2.9	2.8	3.0	3.9
284.70	5.6	4.9	4.8	5.8
288.59	4.6	4.0	3.9	5.1
293.81	8.4	7.4	6.8	8.4
298.57	4.8	4.5	4.4	5.6
304.18	7.7	7.4	6.9	6.9
305.49	6.3	5.5	5.7	6.2
309.10	4.2	3.6	3.7	4.9
314.43	7.6	7.1	6.3	6.2
317.12	7.0	6.4	5.9	6.0
326.18 <sup>c</sup>	7.1	6.8	6.0	5.1
329.58	5.4	4.6	4.3	4.7
339.03	5.8	5.3	4.7	4.0
343.19	2.5	2.1	2.0	2.2
353.17	3.0	2.4	2.2	1.8

<sup>a</sup>Uncertainties are about  $\pm 5\%$ . <sup>b</sup>Not resolved or not included in the spectral data reported by McQuigg and Calvert.<sup>2</sup> <sup>c</sup>Platt et al.<sup>10</sup> reported a value of  $7.8 \times 10^{-20}$  cm<sup>2</sup> molecule<sup>-1</sup> for this peak.

sorption cross sections. For wavelengths greater than 295 nm, only spectra of formaldehyde at pressures less than 2 Torr were used; for wavelengths between 285 and 298 nm, only spectra of formaldehyde at pressures less than 3 Torr were used; and for wavelengths less than 285 nm, spectra of formaldehyde at pressures less than 9 Torr were used. For these wavelength regions and maximum pressure ranges, the absorbances were linear with pressure.

After the division of the spectra for each pressure was made, average absorption cross sections for formaldehyde were calculated at a wavelength interval of 0.04 nm. For each wavelength bin, the average absorbance value over that interval was first determined. For the 0.04-nm-resolution spectra, this was two data points; for the 0.01-nm-resolution spectra, this was eight data

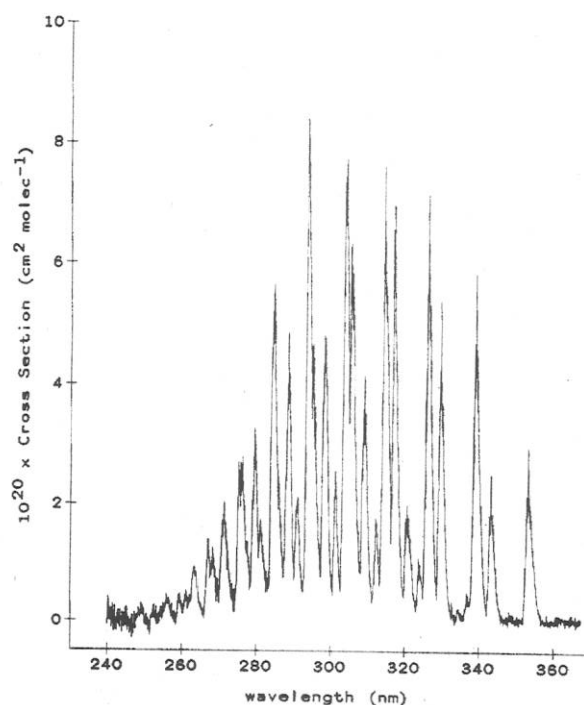


**Figure 3.** Ultraviolet absorption cross sections of HCHO. Data are from least-squares fits to each 0.02-nm interval between 235 and 365 nm. HCHO pressures were less than 2 Torr for wavelengths greater than 295 nm, less than 3 Torr for wavelengths between 285 and 295 nm, and less than 9 Torr for wavelengths less than 285 nm.

**TABLE II: Average UV Absorption Cross Sections of Formaldehyde**

wave- length, <sup>a</sup> nm	$10^{20}\sigma_e$ , cm <sup>2</sup> molecule <sup>-1</sup> (296 K)				
	this work <sup>b</sup>	Calvert et al. <sup>11</sup>	Bass et al. <sup>4</sup>	Moortgat et al. <sup>5c</sup>	Baulch et al. <sup>6</sup>
240	0.011 $\pm$ 0.003				0.03
250	0.103 $\pm$ 0.005				0.13
260	0.440 $\pm$ 0.006				0.47
270	0.903 $\pm$ 0.007		0.93	0.79	0.86
280	1.923 $\pm$ 0.009		1.84	1.88	1.86
290	2.655 $\pm$ 0.016	3.18	2.37	2.65	2.51
300	2.788 $\pm$ 0.022	3.25	2.41	2.83	2.62
310	2.619 $\pm$ 0.026	3.14	2.25	2.65	2.45
320	1.816 $\pm$ 0.019	2.34	1.64	2.06	1.85
330	1.896 $\pm$ 0.025	2.36	1.48	2.04	1.76
340	1.339 $\pm$ 0.016	1.97	0.88	1.48	1.18
350	0.491 $\pm$ 0.007	0.837	0.32	0.52	0.42
360	0.054 $\pm$ 0.004	0.18			0.06

<sup>a</sup>All cross sections averaged for 10-nm intervals centered on the indicated wavelength. <sup>b</sup>Uncertainties are the  $2\sigma$  scatter about the least-squares lines. We estimate that systematic errors in the pressure measurements increase the uncertainties to 1–2%. <sup>c</sup>Not computed in this form by Moortgat et al.<sup>5</sup> However, Baulch et al.<sup>6</sup> computed the mean of the data of Moortgat et al.<sup>5</sup> and Bass et al.<sup>4</sup> From this mean and the data of Bass et al.,<sup>4</sup> average cross sections for the data of Moortgat et al.<sup>5</sup> were computed.

points. The cross sections were then calculated from the slopes of the least-square lines. Figure 3 shows the results of these fits. The band intensity (base *e*) determined from Figure 3 is  $(1.70 \pm 0.03) \times 10^{-18}$  nm cm<sup>2</sup> molecule<sup>-1</sup>. Table I lists the peak absorption cross sections measured for the major absorption bands of formaldehyde.

Average absorption cross sections were also calculated for 0.5- and 10-nm intervals, by use of the same method as above. Table II lists the absorption cross sections calculated in this manner by averaging over 10-nm intervals. A supplementary Appendix listing the absorption cross sections averaged over every 0.5-nm bin is available on request (see paragraph at end of paper regarding availability of supplementary material). The uncertainties calculated from the least-squares fits for the 10-nm intervals from 260 to 350 nm range from 0.5% to 1.4%, with the larger uncer-



ainties calculated for wavelengths greater than 300 nm, for which there were fewer samples due to the need to restrict the pressures to less than 2 Torr.

## Discussion

If the spectral line widths of a molecule are narrower than the resolution used to measure the lines, the absorbance can be nonlinear with pressure; this results in errors in the measured cross sections. Moortgat et al.<sup>9</sup> reported nonlinear absorbances for some absorption bands of formaldehyde, using a resolution of 5 nm. One potential concern is whether the resolutions of 0.04 and 0.01 nm used here are sufficient to accurately measure the cross sections of formaldehyde. Our combined infrared and ultraviolet measurements addressed this question by providing a comparison between the low-pressure measurements in the 99-cm cell and the atmospheric pressure measurements in the 10-cm cell.

Figure 2 includes the results of the combination of IR and UV measurements on formaldehyde for the 10-nm interval centered on 330 nm. The figure shows curvature for the measurements made at low total pressure as the formaldehyde pressure increases. However, the points from the combined IR and UV measurements made at atmospheric pressure fall close to a linear extrapolation of the line determined by the data for which the pressure was less than 2 Torr in the direct pressure measurements. Apparently, the pressure broadening is sufficient at 1-atm total pressure to produce formaldehyde absorbances linear with formaldehyde pressure up to at least 11 Torr. The combination IR and UV measurements show much more scatter because the UV absorbances in the 10-cm cell were only about 0.1–0.2 (base 10) and the signal-to-noise ratio for such small absorbances was quite poor. For this reason, the measurements combining IR and UV data were not used in the final data analysis.

The absorption coefficients for peak wavelengths measured in this work for formaldehyde are compared with literature values in Table I. For wavelengths less than 300 nm, the values measured here vary randomly compared to the literature values. Our values for the peak absorption cross sections tend to be larger than the literature values for wavelengths longer than about 300 nm. This is probably a result of higher resolution (0.04 and 0.01 nm) used in this study. Moortgat et al.<sup>9</sup> found that the cross sections decreased with increasing formaldehyde pressure at a number of wavelengths for a resolution of 5 nm. McQuigg and Calvert<sup>2</sup> measured absorption coefficients of formaldehyde using 1-nm resolution. Moortgat et al.<sup>5</sup> used 0.5-nm resolution, and Bass et al.<sup>4</sup> used 0.05-nm resolution. Platt et al.<sup>10</sup> reported a single absorption coefficient of  $7.8 \times 10^{-20} \text{ cm}^2 \text{ molecule}^{-1}$  at 326.18 nm at a resolution of 0.3 nm.

Table II compares our results for 10-nm averaged cross sections over the 240–360-nm range with the data of Moortgat et al.,<sup>5</sup> Calvert et al.,<sup>11</sup> Bass et al.,<sup>4</sup> and the recommendations by Baulch et al.<sup>6</sup> Our values are 14–70% smaller than the cross sections reported by Calvert et al.<sup>11</sup> for the 290–340-nm region, with the largest disagreement at the longer wavelengths. The sum of the 10-nm averaged cross sections measured here for the 290–360-nm region is 21% smaller than the sum measured by Calvert et al.<sup>11</sup> for this region. At wavelengths longer than 300 nm, our values are 16–53% larger than the values reported by Bass et al.,<sup>4</sup> and the sum of our values for the 270–350-nm region is 16% larger than the sum they measured. The cross sections reported by Moortgat et al.<sup>5</sup> are generally close to our results; our values range from 12% smaller to 14% larger than their values. The sum we measured for the 270–350-nm region is only 3% smaller than the sum measured by Moortgat et al.<sup>5</sup> Our 10-nm averaged cross sections yield a band intensity of  $1.70 \times 10^{-18} \text{ nm cm}^2 \text{ molecule}^{-1}$ , which is about 5% higher than the band intensity of  $1.62 \times 10^{-18} \text{ nm cm}^2 \text{ molecule}^{-1}$  calculated from the 10-nm averaged cross

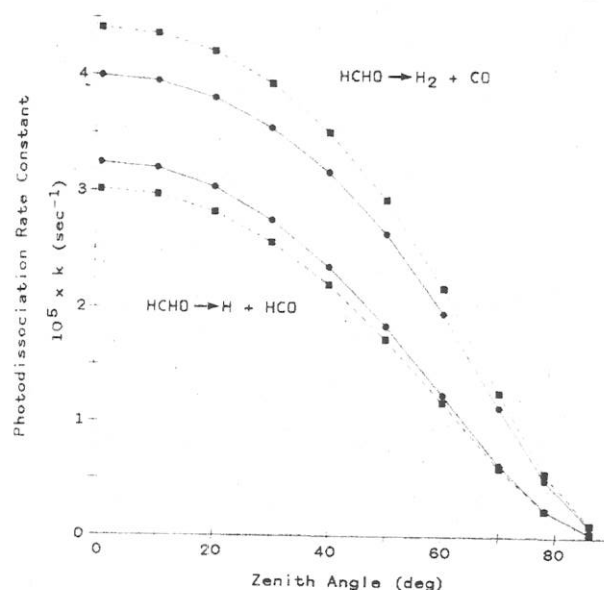


Figure 4. Atmospheric photodissociation rate constants for HCHO vs solar zenith angle for this work (—●—) and for DeMore et al.<sup>7</sup> (---●---). The top two curves compare results for the  $\phi_2$  channel ( $\text{HCHO} \rightarrow \text{H}_2 + \text{CO}$ ), and the bottom two curves compare results for the  $\phi_1$  channel ( $\text{HCHO} \rightarrow \text{H} + \text{HCO}$ ).

sections recommended by Baulch et al.<sup>6</sup>

The photolysis channel of formaldehyde producing  $\text{HO}_2$  radicals and CO becomes more important in the atmosphere at wavelengths longer than 300 nm. In this wavelength region of 300 nm and longer, the sum of our 10-nm averaged cross sections is about 6% larger than that recommended by Baulch et al.<sup>6</sup> Except for the 10-nm interval centered on 240 nm, the recommended cross sections differ from our values by 2–26%.

To assess the affect of these new absorption coefficients of formaldehyde on atmospheric chemistry, atmospheric photodissociation rate constants for formaldehyde were calculated from the relationship<sup>12</sup>

$$k_i(\theta) = \int \sigma(\lambda) I(\theta, \lambda) \phi_i(\lambda) d\lambda$$

where  $k_i(\theta)$  is the photodissociation rate constant for photolytic channel  $i$  at a solar zenith angle  $\theta$ ,  $\sigma(\lambda)$  is the absorption cross section as a function of wavelength  $\lambda$ ,  $I(\theta, \lambda)$  is the spherically integrated actinic flux as a function of solar zenith angle and wavelength, and  $\phi_i(\lambda)$  is the quantum efficiency of channel  $i$  as a function of wavelength.

The photodissociation rate constants as a function of zenith angle were calculated for each photolysis channel of formaldehyde by summing the product of the absorption cross section, the actinic flux, and the quantum yield in that reaction channel for every 0.5-nm increment in wavelength between 290.0 and 365.0 nm. The spherically integrated actinic flux values were taken from Demerjian et al.<sup>12</sup> for their best estimate of the surface albedo and were interpolated to a resolution of 0.5 nm to match the absorption cross sections. The curves recommended by Baulch et al.<sup>6</sup> for the quantum yields of the two reaction channels  $\phi_1$  ( $\text{H} + \text{HCO}$ ) and  $\phi_2$  ( $\text{H}_2 + \text{CO}$ ) as a function of wavelength were used to calculate quantum yields for the two photolysis channels at an interval spacing of 0.5 nm. These recommendations are from the cross sections reported by Horowitz and Calvert,<sup>13</sup> Clark et al.,<sup>14</sup> Tang et al.,<sup>15</sup> Moortgat and Warneck,<sup>16</sup> and Moortgat and

(9) Moortgat, G. K.; Seiler, W.; Warneck, P. *J. Chem. Phys.* **1983**, *78*, 1185.

(10) Platt, U.; Perner, D.; Patz, D. *J. Geophys. Res.* **1979**, *84*, 6329.

(11) Calvert, J. G.; Kerr, J. A.; Demerjian, K. L.; McQuigg, R. D. *Science* **1972**, *175*, 751.

(12) Demerjian, K. L.; Schere, K. L.; Peterson, J. T. *Adv. Environ. Sci. Technol.* **1980**, *10*, 369.

(13) Horowitz, A.; Calvert, J. G. *Int. J. Chem. Kinet.* **1978**, *10*, 805.

(14) Clark, J. H.; Moore, C. B.; Nogar, N. S. *J. Chem. Phys.* **1978**, *68*, 1264.

(15) Tang, K. Y.; Fairchild, P. W.; Lee, E. K. C. *J. Phys. Chem.* **1979**, *83*, 569.

(16) Moortgat, G. K.; Warneck, P. *J. Chem. Phys.* **1979**, *70*, 3639.

TABLE III: Atmospheric Photodissociation Rate Constants for Formaldehyde

zenith angle, deg	$10^5 k, \text{s}^{-1}$			
	10 nm		0.5 nm	
	$\phi_1$	$\phi_2$	$\phi_1$	$\phi_2$
0	3.14	4.79	3.25	3.99
10	3.09	4.74	3.20	3.95
20	2.94	4.57	3.03	3.80
30	2.67	4.27	2.75	3.55
40	2.29	3.82	2.35	3.17
50	1.80	3.19	1.84	2.64
60	1.22	2.37	1.24	1.95
70	0.624	1.38	0.624	1.13
78	0.242	0.613	0.237	0.499
86	0.041	0.127	0.0383	0.1023

<sup>a</sup>Uncertainties are estimated to be about 1–2%, on the basis of the least-squares fits to the cross-section data and an estimate of systematic errors in the pressure measurements.

co-workers.<sup>5,9</sup> These quantum yields gave the same values as those recommended by DeMore et al. (1987) when recalculated at a resolution of 10 nm.

The calculated photodissociation rate constants are listed in Table III. To compare our results with previous calculations, we also calculated the photodissociation rate constants using 10-nm averages for the cross sections, actinic flux, and quantum yields as a function of wavelength. These results are also included in Table III. We found that the resolution of the cross sections used

in the calculations had a significant effect only on the calculated photodissociation rate constants for the  $\phi_2$  channel ( $\text{H}_2 + \text{CO}$ ). For example, at a zenith angle of  $0^\circ$ , the photodissociation rate constant for  $\phi_2$  was 17% lower using the 0.5-nm averaged cross sections rather than the 10-nm averaged cross sections, but the photodissociation rate constant for  $\phi_1$  increased by only 3%. The effect of the increased resolution of 0.5 nm in the calculations is to decrease the photodissociation rate constant for  $\phi_2$ , while the effect of the larger cross sections measured here is to increase this photodissociation rate constant.

Figure 4 compares our results with those calculated from the cross sections recommended by DeMore et al.<sup>7</sup> Our values for the photodissociation rate constant for channel  $\phi_1$  varies from 8% larger than the recommended value at a zenith angle of  $0^\circ$  down to 2% lower at a zenith angle of  $86^\circ$ . Our values for the photodissociation rate constant for channel  $\phi_2$  are about 9–11% lower than the recommended values.

More free radicals ( $\text{HO}_2$ ) will be formed in model calculations of atmospheric chemistry using our new photodissociation rate constants, since we find that more formaldehyde photolyzed into the  $\text{H} + \text{HCO}$  channel than was previously thought. Although detailed atmospheric modeling is required to determine the exact effect on ozone of these results, the general effect will be to increase the calculated amount of ozone formed.

**Supplementary Material Available:** Appendix consisting of a table listing UV absorption coefficients averaged every 0.5 nm (6 pages). Ordering information is given on any current masthead page.

## Resonance Raman Studies of Guanidinium and Substituted Guanidinium Ions

Roseanne J. Sension, Bruce Hudson,\*

Department of Chemistry, University of Oregon, Eugene, Oregon 97403

and Patrik R. Callis

Department of Chemistry, Montana State University, Bozeman, Montana 59717 (Received: October 10, 1989)

Resonance Raman spectra of aqueous solutions of guanidinium, methylguanidinium, 1,1-dimethylguanidinium, ethylguanidinium, and L-arginine salts are reported. The results are interpreted in terms of excited electronic state symmetries and geometry changes with the help of semiempirical INDO/S calculations. The low-lying  $E'(\pi\pi^*)$  excited state of guanidinium exhibits a linear Jahn–Teller distortion along the  $e' \text{CN}_3$  stretching nuclear coordinate. The resonance Raman spectra also indicate a significant force constant change, possibly even a double minimum potential, along the  $\text{CN}_3$  umbrella coordinate in the excited electronic state. The  $\pi \rightarrow \pi^*$  transitions of guanidinium and of all of the substituted guanidinium ions involve charge transfer between the nitrogen atoms and the central carbon atom. In the ground state, the positive charge is shared by the carbon atom and all three of the nitrogen atoms. In the excited electronic state, the carbon atom has a net negative charge. The resonance Raman spectra of all of the substituted guanidinium ions are characterized primarily by a strong enhancement in the intensity of a band located at approximately  $1650 \text{ cm}^{-1}$  ( $1620 \text{ cm}^{-1}$  in the deuterated species). This band is assigned to the fundamental vibrational transition in the asymmetric  $\text{CN}_3$  stretching coordinate involving the symmetric C–N stretching of the unsubstituted nitrogen atoms.

### Introduction

Guanidinium ion,  $(\text{C}(\text{NH}_2)_3)^+$ , is a simple 10-atom species that has been of much interest to biochemists due to its presence as the functional group of the amino acid arginine and its presence as a constituent in other biologically active molecules, and because of its use as a protein denaturant. This species has, however, received only scant attention from spectroscopists since the late 1930s. There are relatively few references in the literature on the spectroscopy of this ion for reasons that can be inferred from its properties. Because the ion only exists in aqueous solution (or in other polar solvents) or in the crystalline form, it is not very amenable to infrared (IR) studies, although there are a few IR studies of guanidinium crystals reported.<sup>1,2</sup> Water does not

interfere with Raman spectroscopy and there are several Raman studies of guanidinium reported in the literature, most dating from the late 1930s.<sup>2–7</sup> The electronic spectrum is also of interest because of the high symmetry of guanidinium and the simplicity of its orbital pattern. Unfortunately, guanidinium does not begin

- (1) Angell, C. L.; Shepard, N.; Yamaguchi, A.; Shimanouchi, T.; Miyazawa, T.; Mizushima, S. *Trans. Faraday Soc.* **1957**, *53*, 589.
- (2) Bonner, O. D.; Jordan, C. F. *Spectrochim. Acta* **1976**, *32*, 1243.
- (3) Edsall, J. T. *J. Phys. Chem.* **1937**, *41*, 133.
- (4) Otvos, J. W.; Edsall, J. T. *J. Chem. Phys.* **1939**, *7*, 632.
- (5) Gupta, J. *J. Indian Chem. Soc.* **1936**, *13*, 575.
- (6) Bonner, O. D. *J. Phys. Chem.* **1977**, *81*, 2247.
- (7) Ananthakrishnan, R. *Proc. Indian Acad. Sci. A* **1937**, *5*, 200.